Available online at www.sciencedirect.com
ScienceDirect
Biomaterials 28 (2007) 316–325
Biomaterials
www.elsevier.com/locate/biomaterials

Continuing differentiation of human mesenchymal stem cells and induced chondrogenic and osteogenic lineages in electrospun PLGA nanofiber scaffold

Xuejun Xin, Mohammad Hussain, Jeremy J. Mao*

Department of Biomedical Engineering, Columbia University, College of Dental Medicine, Fu Foundation School of Engineering and Applied Sciences, 630 W. 168 St., – PH7 East CDM, New York, NY 10032, USA

Received 5 June 2006; accepted 22 August 2006
Available online 28 September 2006

Abstract

Nanofibers have recently gained substantial interest for potential applications in tissue engineering. The objective of this study was to determine whether electrospun nanofibers accommodate the viability, growth, and differentiation of human mesenchymal stem cells (hMSCs) as well as their osteogenic (hMSC-Ob) and chondrogenic (hMSC-Ch) derivatives. Poly(D,L-lactide-*co*-glycolide) (PLGA) beads with a PLA:PGA ratio of 85:15 were electrospun into non-woven fibers with an average diameter of 760 ± 210 nm. The average Young's modulus of electrospun PLGA nanofibers was 42 ± 26 kPa, per nanoindentation with atomic force microscopy (AFM). Human MSCs were seeded 1–4 weeks at a density of 2×10^6 cells/mL in PLGA nanofiber sheets. After 2 week culture on PLGA nanofiber scaffold, hMSCs remained as precursors upon immunoblotting with hKL12 antibody. SEM taken up to 7 days after cell seeding revealed that hMSCs, hMSC-Ob and hMSC-Ch apparently attached to PLGA nanofibers. The overwhelming majority of hMSCs was viable and proliferating in PLGA nanofiber scaffolds up to the tested 14 days, as assayed live/dead tests, DNA assay and BrdU. In a separate experiment, hMSCs seeded in PLGA nanofiber scaffolds were differentiated into chodrogenic and osteogenic cells. Histological assays revealed that hMSCs continuously differentiated into chondrogenic cells and osteogenic cells after 2 week incubation in PLGA nanofibers. Taken together, these data represent an original investigation of continuous differentiation of hMSCs into chondrogenic and osteogenic cells in PLGA nanofiber scaffold. Consistent with previous work, these findings also suggest that nanofibers may serve as accommodative milieu for not only hMSCs, but also as a 3D carrier vehicle for lineage specific cells.

Keywords: Nanofibers; Stem cell; Electrospinning; Scaffold; Tissue engineering

1. Introduction

Mesenchymal stem cells (MSCs) have elicited substantial attention because they can be readily isolated, expanded ex vivo and have been used for in vivo tissue engineering [1–5]. Engineered tissue phenotypes from MSCs include osteochondral grafts with both cartilage and bone [3,5–10], adipose tissue [11,12], tendon and ligaments [13–15] and skeletal muscle [5]. Despite the pioneering effort on the use of MSCs in the engineering of several tissue phenotypes, the optimal scaffolds that are capable of influencing and accommodating the growth and differentiation of MSCs are yet to be identified and likely are specific for each application. During native development and wound healing, cells and molecules interact with extracellular matrix (ECM) molecules such as fibrous proteins and glycosaminoglycans. The ECM milieu surrounding the cell has physical and structural features in the nanometer scale, and may affect several aspects of cell behavior such as morphology, adhesion and cytoskeletal arrangements [16–21].

Recently, synthetic materials have been fabricated into nanometer scale structures in attempts to simulate the matrix environment in which seeded cells can be accommodated to proliferate and differentiate towards desired lineages [22–33]. Electrospinning is one of the approaches

*Corresponding author. Tel.: +1 212 305 4475; fax: +1 212 342 0199.
E-mail address: jmao@columbia.edu (J.J. Mao).

0142-9612/$ - see front matter © 2006 Elsevier Ltd. All rights reserved.
doi:10.1016/j.biomaterials.2006.08.042

that allow the fabrication of synthetic materials into fibrous structures in the nanometer scale [31–39]. Nanofibers formed by electrospinning have been shown to mimic the ECM environment to various degrees when cultured with several cell types [40–46]. Poly(D,L-lactide-*co*-glycolide) (PLGA) has been approved for several biomedical applications in humans and widely used as scaffold materials in tissue engineering [47–49]. The porosity and tensile properties of electrospun PLGA nanofibers have been characterized [50]. Osteoblast adhesion has been shown to occur when seeded in PLGA nanofibers [51]. Poly(ε-caprolactone) (PLC) nanofibers accommodated the differentiation of human mesenchymal stem cells (hMSCs) into adipogenic, osteogenic and chondrogenic cells [52]. PLGA nanofibers have been shown to promote the adhesion of interstitial and endothelial cells [53], the growth of fetal pulmonary cells [54] and porcine chondrocytes [55]. A blend mixture of PLGA and PLGA-*b*-PEG-NH_2 supported the adhesion of an osteoblast cell line [41]. Despite these meritorious studies, relatively little is known whether PLGA nanofibers accommodate continuous differentiation of MSCs into osteoblasts and chondrocytes, all of which are cell lineages of particular importance in osteoarthritis. In this report, we determined the growth and differentiation behavior of MSCs and their osteogenic and chondrogenic derivatives seeded in electrospun PLGA nanofibers.

2. Materials and methods

2.1. Electrospun nanofiber fabrication

Commercially available PLGA beads (85:15; PLA:PGA) (Aldrich, Milwaukee, WI, USA) were dissolved in organic solvent mixture of tetrahydrofuran (THF, Sigma, St. Louis, MO, USA) and dimethylformamide (DMF, Fisher Chemicals, Fair Lawn, NJ, USA). The block PLGA copolymer solution was loaded in a 20-mL syringe capped with 18-G needle. An electric field was created with high voltage power supply at 18 kV between the needle (anode) and the rectangular stainless steel plate (collecting plate: 20 × 30 cm as cathode) at a distance of 20 cm (Spellman High Voltage Electronic, Hauppauge, NY, USA). The polymer solution was drawn from the syringe under accurate infusion control pump (Fisher Scientific, Hanover Park, IL, USA) and sprayed onto the target by combined forces of gravity and electrostatic charge [31–39]. Electrospun nanofibers were collected for additional analysis.

2.2. Scanning electron microscopy (SEM) and nanoindentation with atomic force microscopy (AFM)

Morphological structures of electrospun PLGA nanofibers were observed using SEM (HITACHI S-3000N) coated with Platinum by sputter at an accelerating voltage of 10–20 kV prior to and after cell seeding. A subset of electrospun PLGA nanofibers were deposited on a clean glass substrate and a clean metal disk substrate. Individual PLGA nanofibers were separately subjected to imaging and nanoindentation under atomic force microscope (AFM, Veeco-Digital Instruments, Santa Barbara, CA, USA), per our previous approaches [56–59]. Spherical contact tips were applied to indent PLGA nanofibers in contact mode to image and indent the PLGA nanofibers for the determination of Young's modulus per Hertz model per our previous methods [57–59]:

$$E = \frac{2F(1-\nu^2)\pi \tan\theta}{4\delta^2},$$

where F is the load, ν is Poisson's ratio, θ is intender angle of the conical tip and δ is amount of indentation.

2.3. hMSCs and their differentiation into osteogenic and chondrogenic cells

Bone-marrow-derived hMSCs were purchased from AllCells (Berkeley, CA, USA). The donor was a 25 year-old healthy male volunteer without additional identifier. In our previous work, we have isolated hMSCs from multiple donors [5]. In this report, the isolated hMSCs were culture-expanded in monolayer with a cocktail containing Dulbecco's modified Eagle's medium (DMEM, Sigma, St. Louis, MO, USA) supplemented with 10% fetal bovine serum (FBS, Atlanta Biologicals, Lawrenceville, GA, USA) and 1% antibiotic–antimycotic (Atlanta Biologicals, Lawrenceville, GA, USA). The medium was changed every 3 days, with all cultures maintained at 37 °C with 5% CO_2.

Chondrogenic or osteogenic differentiations were induced per our prior methods [5]. First passage hMSCs were treated with chondrogenic supplements containing 10 ng/mL TGF-β3 (RDI, Flanders, NJ, USA) in serum-free DMEM for 2 weeks. This protocol has induced hMSCs into chondrogenic cells per several molecular and mRNA assays in our previous work [5]. For osteogenic differentiation, hMSCs were treated with a cocktail of 100 nM dexamethasone, 10 mM β-glycerophosphate, and 0.05 mM ascorbic acid-2-phosphate (Sigma-Aldrich, St. Louis, MO, USA) per our previous methods. Von Kossa and alkaline phosphatase assays confirmed that hMSCs so treated had been differentiated into osteogenic cells, and also per our previous work [5]. All cell differentiation cultures were incubated in 95% air, 5% CO_2 at 37 °C with corresponding medium changes every 3 days.

2.4. Cell-seeded PLGA nanofiber construct and differentiation

Culture-expanded hMSCs, hMSC-derived osteoblasts and hMSC-derived chondrocytes were trypsinized, counted and seeded separately into pre-wetted and ethylene oxide sterilized PLGA nanofiber sheets (10 × 10 × 0.5 mm) at a density of 2×10^6 cells/mL. hMSC-seeded PLGA nanofiber constructs were continuously cultured in DMEM supplemented with 10% FBS and 1% antibiotic–antimycotic, as described above. hMSC-derived chondrocytes seeded in PLGA nanofiber constructs were continuously cultured in DMEM supplemented with 10 ng/mL TGF-β3, as described above. hMSC-derived osteoblasts seeded in PLGA nanofiber constructs were continuously cultured in DMEM supplemented with 100 nM dexamethasone, 10 mM β-glycerophosphate, and 0.05 mM ascorbic acid-2-phosphate as described above. All cultures were incubated in corresponding medium for 1, 3 or 7 days. PLGA nanofiber sheets without cell seeding were used as controls.

2.5. Cell morphology in PLGA nanofiber scaffold

Cell-seeded PLGA nanofiber constructs were harvested and washed by PBS and subsequently fixed in 4% glutaraldehyde before dehydration with increasing concentrations of ethanol, and finally with hexamethyldisilazane (HMDS; Fluka Chemical, Milwaukee, WI, USA) to further extract water. The dehydrated, cell-seeded or cell-free PLGA nanofiber constructs were maintained in desiccators equipped with a vacuum for overnight air drying. After sputter-coating with Platinum, SEM was used to observe cell and scaffold morphology and cell attachment on PLGA nanofiber scaffold.

2.6. DNA content, cell viability and cell proliferation assays

PLGA nanofiber scaffolds seeded with hMSCs were incubated for 1, 3, 7 or 14 days. At each time point, cell-seeded and cell-free PLGA scaffolds were sonicated to extract total DNA. DNA content was measured using Hoechst 33258 and DNA quantitation kit and VersaFluor^{TM} Fluorometer System (Bio-Rad, Hercules, CA, USA). Cell viability in PLGA nanofiber scaffolds was determined for cells seeded on the surface of PLGA nanofibers by live/dead viability/cytotoxicity kit (Molecular Probes, L-3224, Eugene, OR, USA) per our previous methods [6]. Green fluorescence by calcein reaction with intracellular esterase indicated live cells, whereas red fluorescence reacted with ethidium homodimer that binds to nucleic acids indicated dead cells. Bromodeoxyuridine (BrdU) (Sigma, St. Louis, MO, USA) was used to label mitotic cells in cell-seeded PLGA nanofiber scaffolds, with cell-free scaffolds as controls. BrdU labeling was analyzed by FITC conjugated anti-BrdU immunofluorescence reagent (Becton Dickinson, Franklin Lakes, NJ, USA).

2.7. Histology, immunohistochemistry, and confocal microscopy

Cell-seeded and cell-free PLGA nanofiber sheets were mounted on slides and fixed in 4% phosphate-buffered paraformaldehyde (Sigma). Mounted sections were stained with hematoxylin and eosion (H&E, Sigma). Upon 1 and 7 days following cell seeding, PLGA nanofiber scaffolds were washed in PBS and fixed with 2% paraformaldehyde at room temperature. Cell-seeded PLGA constructs were incubated with hKL12 primary antibody (1:100–1:800, Acris antibodies GmbH) with 0.5% blocking serum. Each sample was rinsed in PBS for 20 min and incubated with a FITC-conjugated rabbit anti-mouse IgG1 secondary antibody (Research Diagnostics, Hercules, CA, USA) in 0.5% serum for 30 min. The immunological fluorescence-stained cell-seeded constructs were mounted and viewed under laser scanning confocal microscope (LSCM, IX70-HLSH100 Fluoview; Olympus, Tokyo, Japan).

2.8. Data analysis and statistics

Student's *t*-tests were used to determine whether DNA contents at 3, 7 and 14 days after the seeding of hMSCs differed from 1 day after seeding at an alpha level of $P<0.05$.

3. Results

3.1. Electrospun PLGA nanofibers and AFM characterization

PLGA nanofibers fabricated by electrospinning in this study showed non-woven mat structures as in SEM images (Fig. 1A and 1B). Fiber orientation was apparently random, with average fiber diameters in the range of 550–970 nm (mean: 760 ± 210 nm: mean $\pm$ standard deviation and thereafter). Topographic imaging by AFM of the electrospun PLGA nanofibers revealed fibrous and regular smooth surface features on either glass or stainless steel surfaces (Fig. 1C and D, respectively) and in three-dimensional observation (Fig. 1E), consistent with the diameter measurements using SEM (Fig. 1A and B). By extracting from force volume images and nanoindentation force curves, and the application of Hertz model, the calculated average Young's modulus of the electrospun PLGA nanofibers was 42 ± 26 kPa.

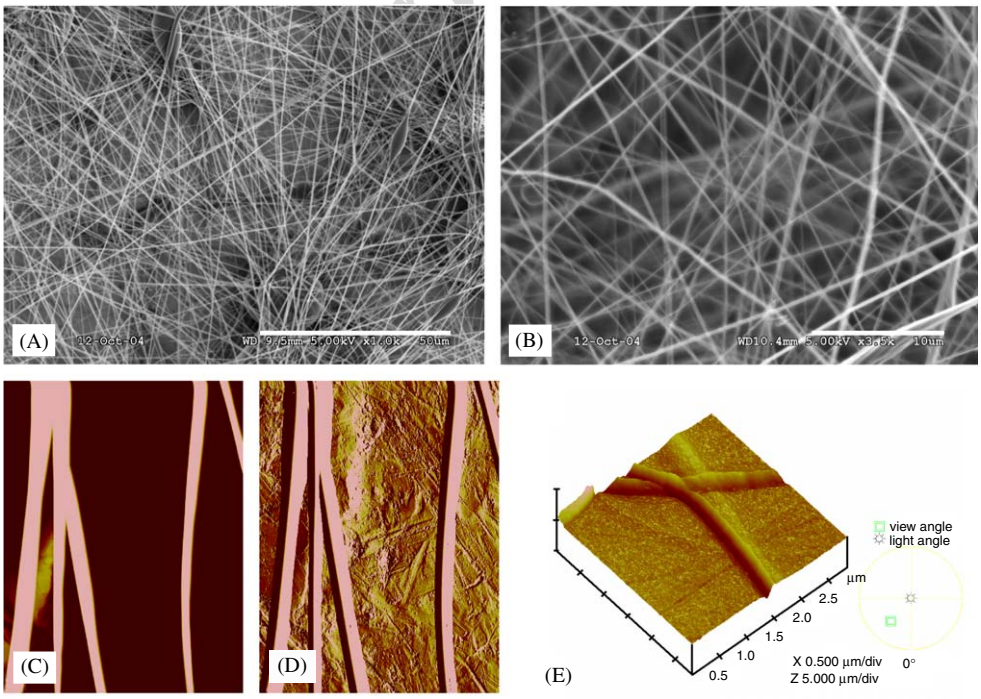

Fig. 1. Electrospun PLGA nanofibers: (A) PLGA nanofibers as non-woven mesh-like structures under SEM. (B) Higher SEM magnification showing irregular pores among PLGA nanofibers. (C) Imaging of single PLGA nanofibers deposited on glass substrate by atomic force microscopy (AFM). (D) AFM imaging of individual PLGA nanofibers on stainless steel substrate. (E) 3D contour of PLGA nanofibers under AFM (scale bars A: 50 μm; B: 10 μm).

3.2. Cell seeding and interactions with PLGA nanofiber scaffold

Near confluent hMSCs were trypsinized, suspended and seeded in electrospun PLGA nanofibers. Live and dead assay revealed that hMSCs in 2D were viable prior to trypsinization (Fig. 2A). Two weeks following the seeding of hMSCs in PLGA nanofibers, live and dead assay showed that the seeded hMSCs in the 3D PLGA nanofiber scaffold were still alive (Fig. 2B). DNA contents of hMSCs seeded in PLGA nanofiber scaffold increased from 1 to 14 days after cell seeding, indicating progressive proliferation of the seeded hMSCs (Fig. 2C). Significantly greater DNA contents were observed after 3, 7 and 14 days after hMSC seeding in comparison with the first day after hMSC seeding (Fig. 2C). BrdU labeling at 14 days after hMSC seeding in electrospun PLGA nanofiber scaffold revealed that a substantial number of the seeded hMSCs were undergoing mitosis (Fig. 2D).

3.3. Cell morphology in electrospun PLGA nanofiber scaffold

Prior to cell seeding, PLGA nanofibers incubated in DMEM (Fig. 3A), osteogenic supplemented DMEM (Fig. 3E) and chondrogenic supplemented DMEM (Fig. 3I) revealed somewhat uniform morphological features such as random orientation, with little difference among them, as expected. However, hMSCs seeded 1, 3 and 7 days in PLGA nanofiber scaffolds and analyzed with SEM showed apparent morphological differences (top row in Fig. 3). Seven days after seeding, hMSCs apparently attached to PLGA nanofibers and penetrated into the pores (Fig. 3D), in comparison with hMSCs seeded for 1 and 3 days (Fig. 3B and C, respectively). One day after seeding, hMSCs appeared somewhat rounded in shape (Fig. 3B), in contrast with a more elongated cell shape 7 days after seeding (Fig. 3D), suggesting that the seeded hMSCs increasingly attach to PLGA nanofibers. The morphology of hMSC-derived osteoblasts seeded in PLGA nanofibers was also remarkable. Seven days after cell seeding, hMSC-Ob apparently elaborated a substantial amount of extracellular matrices (Fig. 3H), in comparison with hMSC-Ob seeded for 1 and 3 days (Fig. 3F and G, respectively) and PLGA nanofibers incubated in osteogenic medium but without cell seeding (Fig. 3E). Similar to hMSCs, hMSC-derived osteoblasts appeared somewhat rounded 1 day after cell seeding (Fig. 3F) in contrast to the more elongated cell shape that appeared 7 days after cell seeding (Fig. 3H), suggesting hMSC-Ob attachment to PLGA nanofibers. Penetration of hMSC-derived chondrocytes into PLGA nanofibers was most apparent 7 days after cell seeding in contrast with those seeded for 1 and 3 days (Fig. 3J–L). Most PLGA nanofibers were still visible

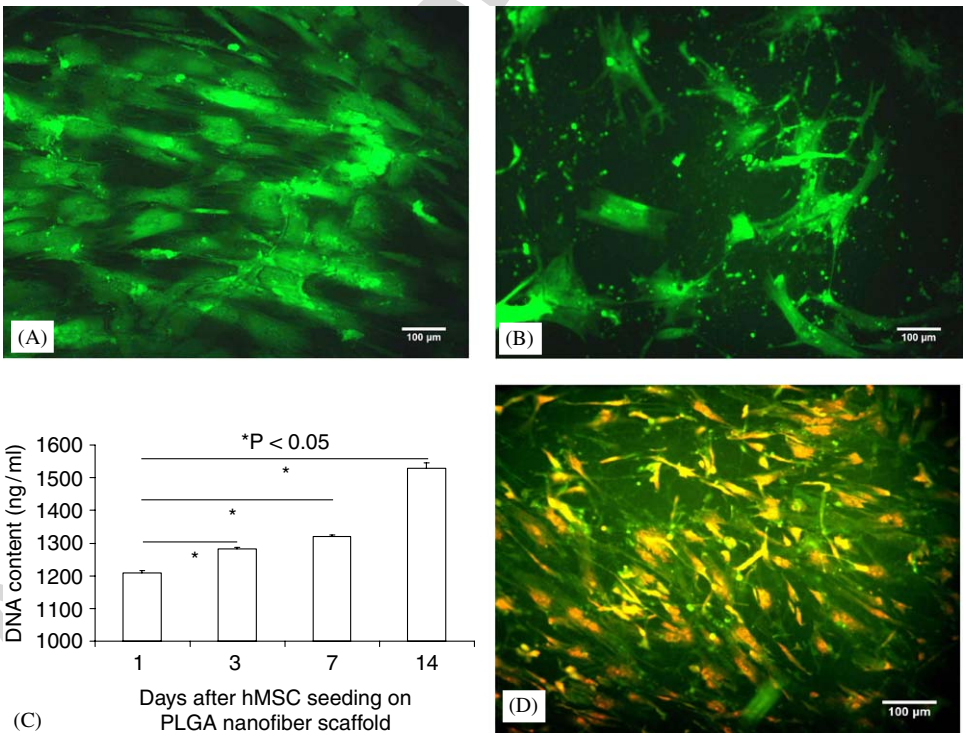

Fig. 2. Human mesenchymal stem cells (hMSCs) and seeding in electrospun PLGA nanofiber scaffold: (A) prior to seeding in nanofiber scaffold, hMSCs in 2D culture were nearly confluent, and were viable by live and dead assay (calcein green indicating live cells). (B) hMSCs seeded in PLGA nanofiber scaffold for 2 weeks showed viability by live and dead assay. (C) DNA contents gradually increased from 1 to 14 days after seeding of hMSCs in PLGA nanofiber scaffold. The DNA contents at each of 3, 7 and 14 days after cell seeding were significantly higher than the DNA content at 1 day following cell seeding. (D) Bromodeoxyuridine (BrdU) immunolocalization showed that a substantial number of seeded hMSCs in nanofiber scaffold were undergoing mitosis (scale bars: 100 μm).

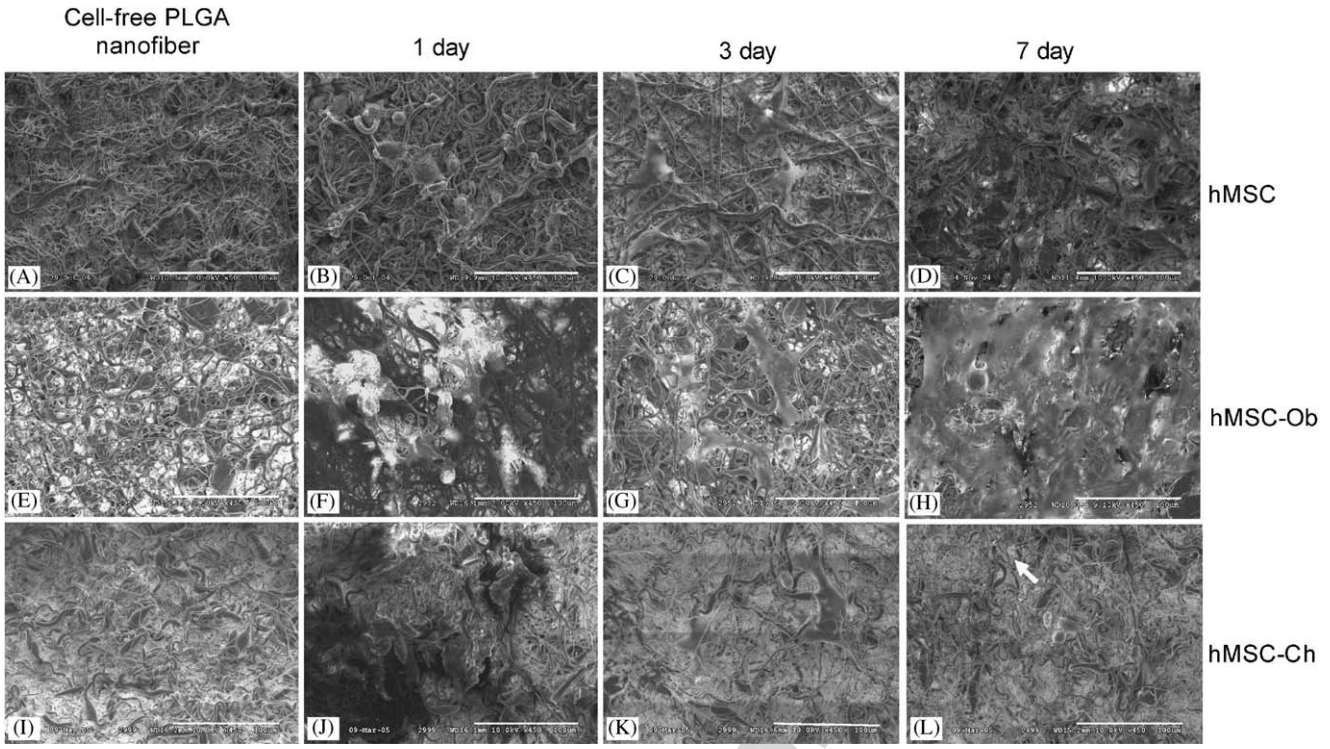

Fig. 3. Electrospun PLGA nanofibers and the seeding of human mesenchymal stem cells (hMSCs), as well as hMSC-derived osteoblasts and hMSC-derived chondrocytes. (A), (E), (I) Prior to cell seeding, three randomly selected PLGA nanofiber scaffolds showed similar characteristics. Upon seeding of hMSCs (B, C, D), various extracellular matrices were apparently synthesized among PLGA nanofibers over time. By 7 days following hMSC seeding, the seeded cells apparently have attached to nanofiber surface and penetrated into the pores of PLGA nanofiber scaffolds (D), in comparison with 1 and 3 days after cell seeding (B and C, respectively). The morphology of hMSC-derived osteoblasts seeded in PLGA nanofibers also varied between 1, 3 and 7 days following cell seeding (F, G, and H, respectively). By 7 days following cell seeding, hMSC-Ob apparently synthesized a substantial amount of extracellular matrices (H), in comparison with 1 and 3 days after cell seeding (F and G, respectively). Human MSC-derived osteoblasts apparently attached to nanofiber substrates. Human MSC-derived chondrocytes revealed characteristic featured after seeding in PLGA nanofibers (J, K and L). Most PLGA nanofibers were still visible at 7 days following the seeding of hMSC-Ch (L), in comparison with the characteristics of hMSC-Ob seeded in PLGA nanofiber scaffolds after 7 days (H). A number of seeded hMSC-Ch apparently was located in lacunae-like structures, seen arrow (L) (scale bar = 100 μm).

7 days after the seeding of hMSC-Ch (Fig. 3L), in comparison with the characteristics of hMSC-Ob seeded in PLGA nanofiber scaffolds for 7 days (Fig. 3H). A number of seeded hMSC-Ch appeared to reside in lacunae-like structures (arrow in Fig. 3L).

3.4. Cell phenotype by histological staining and fluorescence/confocal microscope

H&E staining of hMSCs immediately prior to trypsinization and cell seeding revealed their near confluence and the typical spindle-like morphology (Fig. 4A), similar to our previous work [12]. By Day 7 after cell seeding, hMSCs assumed apparently random orientations among PLGA nanofibers (Fig. 4B). Under confocal microscopy, hMSCs cultured in 2D Petri dishes showed somewhat elongated and spindle shape at 14 days following cell seeding (Fig. 4C). The representative confocal microscopic image of hMSCs seeded in PLGA nanofibers also showed somewhat elongated shape at 14 days following cell seeding (Fig. 4D). The seeded hMSCs apparently attached to PLGA nanofibers (Fig. 4D).

3.5. Differentiation of hMSCs into chondrogenic and osteogenic cells in 3D PLGA nanofibers

hMSCs seeded in PLGA nanofiber scaffold in chondrogenic induced medium began to develop blue color with red nucleated stain from 1 week to 4 weeks with alcian blue staining (Fig. 5D–F). Alcian blue labels glycosaminoglycans and is a conventional marker for chondrogenesis. In comparison, alcian blue staining was negative for hMSCs seeded in PLGA nanofibers without chondrogenic differentiations (Fig. 5A–C). For hMSCs seeded in PLGA nanofibers and treated with osteogenic medium, alizarin red was positive from 1 to 4 weeks (Fig. 5J–L), indicating potential mineral deposition, in comparison with mostly negative alizarin red in hMSCs seeded in PLGA nanofibers without osteogenic differentiation (Fig. 5G–I).

4. Discussion

The present data represent an original report of the differentiation of hMSCs into chondrocytes and osteoblasts in PLGA nanofibers. In a closely related report,

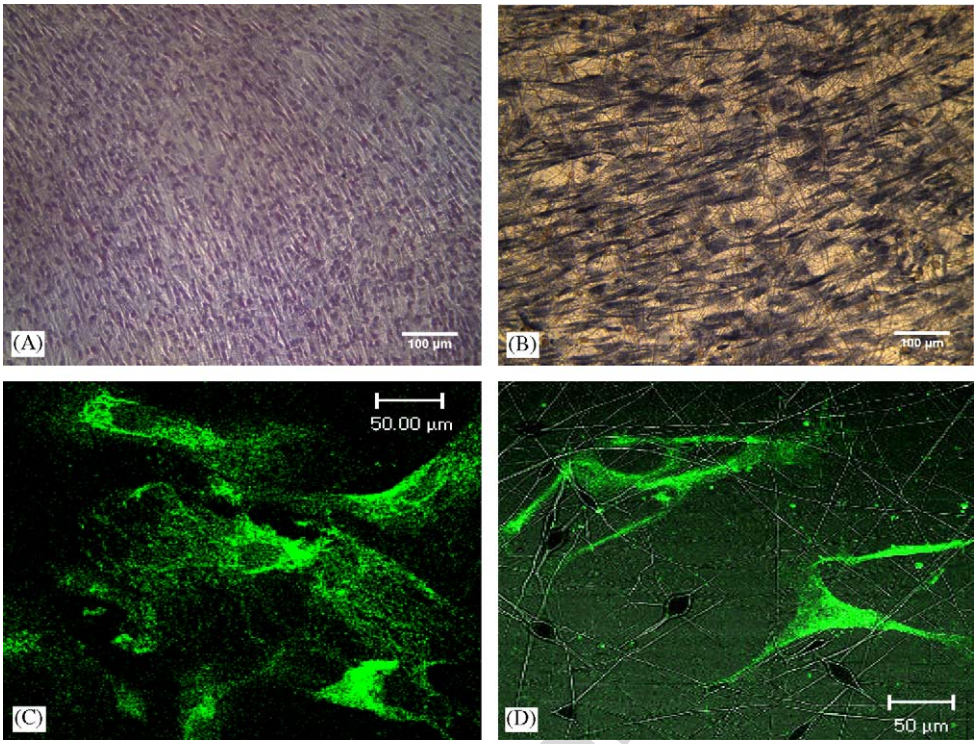

Fig. 4. Imaging of human mesenchymal stem cells (hMSCs) and nanofiber scaffolds. (A) H&E staining of hMSCs in 2D immediately prior to trypsinization and cell seeding. (B) Day 7 after seeding of hMSCs in PLGA nanofibers. (C) Confocal microscopy showing that hMSCs in 2D assumed somewhat elongated and spindle shape at 14 days following cell seeding. (D) Confocal microscopic image of hMSCs seeded in PLGA nanofibers showing somewhat elongated shape at 14 days following cell seeding. The seeded hMSCs apparently attached to PLGA nanofibers. This verifies that hMSC cultured either in 2D or in 3D of PLGA nanofiber consistently maintain stem cell phenotype after 14 days in vitro (scale bars: A, B: 100 μm; C, D: 50 μm).

hMSCs were differentiated into adipocytes, chondrocytes and osteoblasts in PCL nanofibers [52]. PLGA and PCL have a number of different material properties that warrant separate investigations of the differentiation behavior of hMSCs. The present data demonstrate that electrospun PLGA nanofibers are cytocompatible with not only hMSCs, but also osteoblasts and chondrocytes that derive from hMSCs. This is in general consistency with previous work that investigated the cytocompatibility of nanofibers [60–62]. Histological staining demonstrates that the PLGA nanofibers are capable of supporting seeded hMSC to differentiate, maintaining differentiated cell functions. The significantly increasing DNA contents of hMSCs over 14 days of cell seeding suggest that hMSCs continue to proliferate upon seeding in PLGA nanofibers. Thus, PLGA nanofibers apparently accommodate the self-replication of hMSCs. The ability of hMSCs to self-replicate is considered one of the essential properties of stem cells [5,63]. Per SEM and confocal microscopic images shown in the present study, the seeded hMSCs apparently are attached to PLGA nanofibers. One of the advantages of 3D nanofiber systems for seeding hMSCs is that in comparison with 2D culture system, cell seeding in 3D nanofiber system offers substantial surface area-to-volume ratio that maximizes cell–material contact.

Few previous studies have simultaneously investigated the cytocompatibility of hMSCs, hMSC-derived osteoblasts and hMSC-derived chondrocytes. In the present work, hMSCs were shown to have retained their phenotype as precursor cells as shown by hKL12 antibody staining. Further, hMSCs were shown to proliferate by BrdU staining. In addition, hMSC-derived chondrocytes assumed somewhat rounded appearance and resided in lacunae-like structures 7 days following cell seeding. Qualitatively, the morphology of hMSC-derived chondrocytes apparently differs from that of hMSCs and hMSC-derived osteoblasts. This is remarkable in that chondrocytes in native environment elaborate pericellular matrix that is enclosed in a chondron, and separated from neighboring chondrocytes with interterritorial matrix [57,64–66]. The present observation of somewhat rounded hMSC-derived chondrocytes after 7 days of seeding in PLGA nanofibers, in comparison with the morphology of hMSCs and hMSC-derived osteoblasts under the same conditions and at the same cell seeding density, suggests that hMSC-derived chondrocytes may have maintained their lineage characteristics in PLGA nanofiber scaffolds. Additional experiments are warranted to test this speculation. Previous work in cartilage tissue engineering has relied on various hydrogel scaffolds. It is probable that

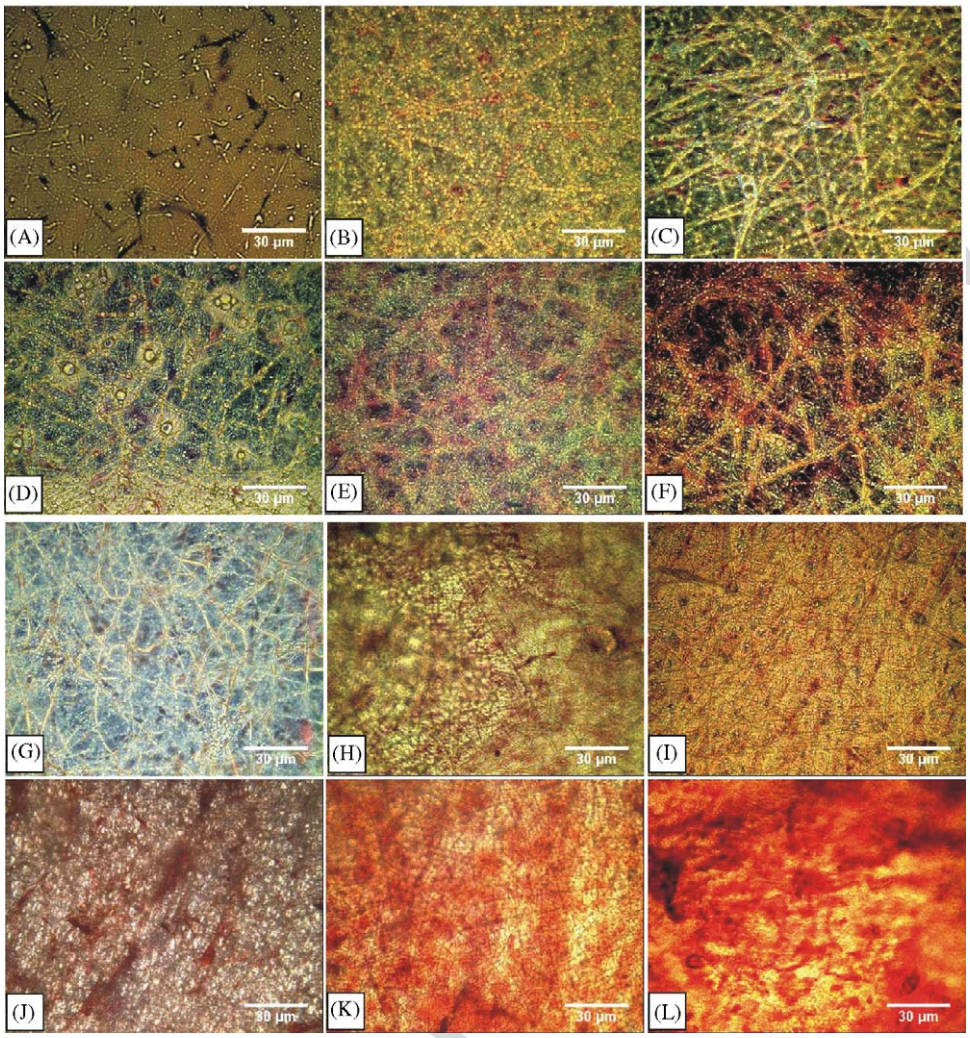

Fig. 5. Differentiation of human mesenchymal stem cells (hMSCs) seeded in PLGA nanofiber scaffold in 3D. (A)–(C) hMSCs cultured in PLGA nanofibers without chondrogenic differentiation showed negative staining to alcian blue, indicating a lack of chondrogenic differentiation. (D)–(F) hMSCs seeded in PLGA nanofibers and treated with chondrogenic medium showed positive staining to alcian blue, suggesting that hMSCs have differentiated into chondrogenic cells with the presence of glycosaminoglycans. (G)–(I) hMSCs cultured in PLGA nanofibers without osteogenic differentiation showed negative staining to alizarin red, indicating a lack of osteogenic differentiation. (J)–(L) hMSCs seeded in PLGA nanofibers and treated with osteogenic medium showed positive staining to alizarin red, suggesting that hMSCs have differentiated into osteogenic cells with the presence of mineral deposition (scale bar: 30 μm).

nanofibers can be either used alone or serve as inserts in hydrogels towards cartilage engineering.

Physical properties and morphological structure of PLGA nanofiber fabricated by electrospinning in this work indicate that the formed scaffold has nanometer scale fibers, elastic property and porous structure. The morphological architecture of PLGA nanofiber scaffold is similar to those of natural ECM [67], suitable to nutrient and metabolic waste exchange. Single PLGA nanofiber has elastic modulus (42 ± 26 kPa) as demonstrated by AFM in this study. The average elastic modulus in this work is similar to the elastic moduli for hMSCs (37 ± 9.62 kPa), hMSC-derived chondrogenic cell (44.85 ± 11.96 kPa) and hMSC-derived osteogenic cells (50.68 ± 3.27), as found in our previous work also by AFM [5]. The similar elastic properties of PLGA nanofibers with hosting cells may be conducive to cell proliferation and differentiation, although this speculation warrants experimental investigations.

Osteoblasts derived from hMSCs in the present study showed morphological features that differ from both hMSCs, and hMSC-derived chondrocytes. Upon 7 days following the seeding in electrospun PLGA nanofibers, hMSC-derived osteoblasts apparently synthesized a substantial amount of matrices and likely penetrated the pores of PLGA nanofibers. Both SEM and confocal microscopy images suggest that hMSC-derived osteoblasts begin to attach to PLGA nanofibers following 1 and 3 days of cell seeding. This is perhaps an indication that the attachment of hMSC-derived osteoblasts is pre-requisite to matrix apposition as seen in the development of native osteoblasts.

The present work elicits a large of number of questions to be addressed in additional studies. Whether cell attachment in PLGA nanofibers is via cell adhesion molecules requires additional studies. At a relatively low cell seeding density and with the assumption and observation that cell–cell contact is not common, whether the seeded cells communicate by paracrine or autocrine pathways is an interesting biological question. The long-term interactions between seeded cells and PLGA nanofiber scaffolds should also be investigated. Degradation of PLGA polymers leads to acidic environment and should be addressed in its effects on seeded cells. This potential issue may be less significant if PLGA nanofibers are used as inserts in other biomaterials such as hydrogel, instead of as a bulk material. Nonetheless, the present data are consistent with previous work and adds that electrospun PLGA nanofiber scaffolds are cytocompatible to not only hMSCs, but also to their osteoblast and chondrocyte lineages. In this work, hMSCs were obtained from a single adult donor. We have previously utilized multiple donors and obtained similar results [68,69]. Although certain inter-donor variability is expected, our previous observation indicates that hMSCs in multiple donors can be differentiated into multiple cell lineages [70].

5. Conclusion

PLGA nanofiber scaffolds accommodate continuous differentiation of hMSCs into osteoblasts and chondrocytes. We confirm that PLGA nanofibers accommodate the survival and proliferation of hMSCs. hMSCs, as well as hMSC-derived chondrogenic and osteogenic cells apparently attach to PLGA nanofibers, and yet assume apparently different morphological features.

Acknowledgements

This research was supported by NIH Grants DE16338 to X.J.X., and DE15391 and EB02332 to J.J.M.

References

[1] Colter DC, Sekiya I, Prockop DJ. Identification of a subpopulation of rapidly self-renewing and multipotential adult stem cells in colonies of human marrow stromal cells. Proc Natl Acad Sci USA 2001;98(14):7841–5.
[2] Jiang Y, Jahagirdar BN, Reinhardt RL, Schwartz RE, Keene CD, Ortiz-Gonzalez XR, et al. Pluripotency of mesenchymal stem cells derived from adult marrow. Nature 2002;418(6893):41–9.
[3] Pittenger MF, Mackay AM, Beck SC, Jaiswal RK, Douglas R, Mosca JD, et al. Multilineage potential of adult human mesenchymal stem cells. Science 1999;284(5411):143–7.
[4] Shake JG, Gruber PJ, Baumgartner WA, Senechal G, Meyers J, Redmond JM, et al. Mesenchymal stem cell implantation in a swine myocardial infarct model: engraftment and functional effects. Ann Thorac Surg 2002;73(6):1919–25 [discussion 26].
[5] Alhadlaq A, Mao JJ. Mesenchymal stem cells: isolation and therapeutics. Stem Cells Dev 2004;13(4):436–48.
[6] Alhadlaq A, Elisseeff JH, Hong L, Williams CG, Caplan AI, Sharma B, et al. Adult stem cell driven genesis of human-shaped articular condyle. Ann Biomed Eng 2004;32(7):911–23.
[7] Martin I, Shastri VP, Padera RF, Yang J, Mackay AJ, Langer R, et al. Selective differentiation of mammalian bone marrow stromal cells cultured on three-dimensional polymer foams. J Biomed Mater Res 2001;55(2):229–35.
[8] Mackay AM, Beck SC, Murphy JM, Barry FP, Chichester CO, Pittenger MF. Chondrogenic differentiation of cultured human mesenchymal stem cells from marrow. Tissue Eng 1998;4(4):415–28.
[9] Johnstone B, Hering TM, Caplan AI, Goldberg VM, Yoo JU. In vitro chondrogenesis of bone marrow-derived mesenchymal progenitor cells. Exp Cell Res 1998;238(1):265–72.
[10] Calvert JW, Marra KG, Cook L, Kumta PN, DiMilla PA, Weiss LE. Characterization of osteoblast-like behavior of cultured bone marrow stromal cells on various polymer surfaces. J Biomed Mater Res 2000;52(2):279–84.
[11] Stosich MS, Mao JJ. Stem cell based soft tissue grafts for plastic and reconstructive surgeries. Seminars in Plastic Surgery 2005;19:251–60.
[12] Alhadlaq A, Tang M, Mao JJ. Engineered adipose tissue from human mesenchymal stem cells maintains predefined shape and dimension: implications in soft tissue augmentation and reconstruction. Tissue Eng 2005;11(3–4):556–66.
[13] Risbud MV, Shapiro IM. Stem cells in craniofacial and dental tissue engineering. Orthod Craniofac Res 2005;8(2):54–9.
[14] Noth U, Schupp K, Heymer A, Kall S, Jakob F, Schutze N, et al. Anterior cruciate ligament constructs fabricated from human mesenchymal stem cells in a collagen type I hydrogel. Cytotherapy 2005;7(5):447–55.
[15] Beyer Nardi N, da Silva Meirelles L. Mesenchymal stem cells: isolation, in vitro expansion and characterization. Handbook Exp Pharmacol 2006;174:249–82.
[16] Yim EK, Reano RM, Pang SW, Yee AF, Chen CS, Leong KW. Nanopattern-induced changes in morphology and motility of smooth muscle cells. Biomaterials 2005;26(26):5405–13.
[17] Wan Y, Wang Y, Liu Z, Qu X, Han B, Bei J, et al. Adhesion and proliferation of OCT-1 osteoblast-like cells on micro- and nano-scale topography structured poly(L-lactide). Biomaterials 2005;26(21):4453–9.
[18] Sniadecki NJ, Desai RA, Ruiz SA, Chen CS. Nanotechnology for cell–substrate interactions. Ann Biomed Eng 2006;34(1):59–74.
[19] Miller DC, Thapa A, Haberstroh KM, Webster TJ. Endothelial and vascular smooth muscle cell function on poly(lactic-*co*-glycolic acid) with nano-structured surface features. Biomaterials 2004;25(1):53–61.
[20] Lee CH, Shin HJ, Cho IH, Kang YM, Kim IA, Park KD, et al. Nanofiber alignment and direction of mechanical strain affect the ECM production of human ACL fibroblast. Biomaterials 2005;26(11):1261–70.
[21] Andersson AS, Brink J, Lidberg U, Sutherland DS. Influence of systematically varied nanoscale topography on the morphology of epithelial cells. IEEE Trans Nanobiosci 2003;2(2):49–57.
[22] Noh HK, Lee SW, Kim JM, Oh JE, Kim KH, Chung CP, et al. Electrospinning of chitin nanofibers: degradation behavior and cellular response to normal human keratinocytes and fibroblasts. Biomaterials 2006;27(21):3934–44.
[23] Chua KN, Lim WS, Zhang P, Lu H, Wen J, Ramakrishna S, et al. Stable immobilization of rat hepatocyte spheroids on galactosylated nanofiber scaffold. Biomaterials 2005;26(15):2537–47.
[24] He W, Ma Z, Yong T, Teo WE, Ramakrishna S. Fabrication of collagen-coated biodegradable polymer nanofiber mesh and its potential for endothelial cells growth. Biomaterials 2005;26(36):7606–15.
[25] Ma Z, He W, Yong T, Ramakrishna S. Grafting of gelatin on electrospun poly(caprolactone) nanofibers to improve endothelial cell spreading and proliferation and to control cell orientation. Tissue Eng 2005;11(7–8):1149–58.

[26] Venugopal J, Ma LL, Yong T, Ramakrishna S. In vitro study of smooth muscle cells on polycaprolactone and collagen nanofibrous matrices. Cell Biol Int 2005;29(10):861–7.
[27] Ma Z, Kotaki M, Yong T, He W, Ramakrishna S. Surface engineering of electrospun polyethylene terephthalate (PET) nanofibers towards development of a new material for blood vessel engineering. Biomaterials 2005;26(15):2527–36.
[28] Rahaman MN, Mao JJ. Stem cell-based composite tissue constructs for regenerative medicine. Biotechnol Bioeng 2005;91(3):261–84.
[29] Venugopal J, Ramakrishna S. Applications of polymer nanofibers in biomedicine and biotechnology. Appl Biochem Biotechnol 2005; 125(3):147–58.
[30] Zhang YZ, Venugopal J, Huang ZM, Lim CT, Ramakrishna S. Characterization of the surface biocompatibility of the electrospun PCL-collagen nanofibers using fibroblasts. Biomacromolecules 2005;6(5):2583–9.
[31] Reneker DHCI. Nanometre diameter fibers of polymer, produced by electrospinning. Nanotechnology 1996;7:216–23.
[32] Doshi JRD. Electrospinning process and application of electrospun fibers. J Electrostat 1995;35:151–60.
[33] Baumgartner P. Electrostatic spinning of acrylic microfibers. J Colloid Interface Sci 1971;36:71–9.
[34] Nair LS, Bhattacharyya S, Laurencin CT. Development of novel tissue engineering scaffolds via electrospinning. Expert Opin Biol Ther 2004;4(5):659–68.
[35] Ko FKBM, Laurencin CT. The role of fiber architecture in biocomposites: the tissue engineering approach. In: Proceedings of the 13th international conference on composite materials, 2001.
[36] Chun IRD, Fong H, Fang X. Carbon nanofibers from polyacrylonitrile and mesophase pitch. J Adv Mater 1999;31:36–41.
[37] Fong HCI, Reneker DH. Beaded nanofibers formed during electrospinning. Polymer 1999;40:4585–92.
[38] Kim JRD. Mechanical properties of composites using ultrafine electrospun fibers. Polym Compos 1999;20:124–31.
[39] Ko FKLC, Borden MD, Reneker DH. The dynamics of cell–fiber architecture interaction. In: Proceedings of the Annual Meeting of the Biomaterials Research Society, vol. 11. 1998.
[40] Badami AS, Kreke MR, Thompson MS, Riffle JS, Goldstein AS. Effect of fiber diameter on spreading, proliferation, and differentiation of osteoblastic cells on electrospun poly(lactic acid) substrates. Biomaterials 2006;27(4):596–606.
[41] Kim TG, Park TG. Biomimicking extracellular matrix: cell adhesive RGD peptide modified electrospun poly(D,L-lactic-*co*-glycolic acid) nanofiber mesh. Tissue Eng 2006;12(2):221–33.
[42] Kidoaki S, Kwon IK, Matsuda T. Mesoscopic spatial designs of nano- and microfiber meshes for tissue-engineering matrix and scaffold based on newly devised multilayering and mixing electrospinning techniques. Biomaterials 2005;26(1):37–46.
[43] Ma Z, Kotaki M, Inai R, Ramakrishna S. Potential of nanofiber matrix as tissue-engineering scaffolds. Tissue Eng 2005;11(1–2): 101–9.
[44] Schindler M, Ahmed I, Kamal J, Nur EKA, Grafe TH, Young Chung H, et al. A synthetic nanofibrillar matrix promotes in vivo-like organization and morphogenesis for cells in culture. Biomaterials 2005;26(28):5624–31.
[45] Mo XM, Xu CY, Kotaki M, Ramakrishna S. Electrospun P(LLA-CL) nanofiber: a biomimetic extracellular matrix for smooth muscle cell and endothelial cell proliferation. Biomaterials 2004;25(10): 1883–90.
[46] Xu C, Inai R, Kotaki M, Ramakrishna S. Electrospun nanofiber fabrication as synthetic extracellular matrix and its potential for vascular tissue engineering. Tissue Eng 2004;10(7–8):1160–8.
[47] Agrawal CM, Ray RB. Biodegradable polymeric scaffolds for musculoskeletal tissue engineering. J Biomed Mater Res 2001;55(2): 141–50.
[48] Behravesh E, Yasko AW, Engel PS, Mikos AG. Synthetic biodegradable polymers for orthopaedic applications. Clin Orthop Relat Res 1999;367(Suppl.):S118–29.
[49] Athanasiou KA, Niederauer GG, Agrawal CM. Sterilization, toxicity, biocompatibility and clinical applications of polylactic acid/polyglycolic acid copolymers. Biomaterials 1996;17(2):93–102.
[50] Li WJ, Laurencin CT, Caterson EJ, Tuan RS, Ko FK. Electrospun nanofibrous structure: a novel scaffold for tissue engineering. J Biomed Mater Res 2002;60(4):613–21.
[51] Price RL, Ellison K, Haberstroh KM, Webster TJ. Nanometer surface roughness increases select osteoblast adhesion on carbon nanofiber compacts. J Biomed Mater Res A 2004;70(1):129–38.
[52] Li WJ, Tuli R, Huang X, Laquerriere P, Tuan RS. Multilineage differentiation of human mesenchymal stem cells in a three-dimensional nanofibrous scaffold. Biomaterials 2005;26(25):5158–66.
[53] Telemeco TA, Ayres C, Bowlin GL, Wnek GE, Boland ED, Cohen N, et al. Regulation of cellular infiltration into tissue engineering scaffolds composed of submicron diameter fibrils produced by electrospinning. Acta Biomater 2005;1(4):377–85.
[54] Mondrinos MJ, Koutzaki S, Jiwanmall E, Li M, Dechadarevian JP, Lelkes PI, et al. Engineering three-dimensional pulmonary tissue constructs. Tissue Eng 2006;12(4):717–28.
[55] Shin HJ, Lee CH, Cho IH, Kim YJ, Lee YJ, Kim IA, et al. Electrospun PLGA nanofiber scaffolds for articular cartilage reconstruction: mechanical stability, degradation and cellular responses under mechanical stimulation in vitro. J Biomater Sci Polym Ed 2006;17(1–2):103–19.
[56] Clark PA, Rodriguez A, Sumner DR, Hussain MA, Mao JJ. Modulation of bone ingrowth of rabbit femur titanium implants by in vivo axial micromechanical loading. J Appl Physiol 2005; 98(5):1922–9.
[57] Allen DM, Mao JJ. Heterogeneous nanostructural and nanoelastic properties of pericellular and interterritorial matrices of chondrocytes by atomic force microscopy. J Struct Biol 2004;145(3):196–204.
[58] Patel RV, Mao JJ. Microstructural and elastic properties of the extracellular matrices of the superficial zone of neonatal articular cartilage by atomic force microscopy. Front Biosci 2003;8:a18–25.
[59] Hu K, Radhakrishnan P, Patel RV, Mao JJ. Regional structural and viscoelastic properties of fibrocartilage upon dynamic nanoindentation of the articular condyle. J Struct Biol 2001;136(1):46–52.
[60] Sahoo S, Ouyang H, Goh JC, Tay TE, Toh SL. Characterization of a novel polymeric scaffold for potential application in tendon/ligament tissue engineering. Tissue Eng 2006;12(1):91–9.
[61] Katti DS, Robinson KW, Ko FK, Laurencin CT. Bioresorbable nanofiber-based systems for wound healing and drug delivery: optimization of fabrication parameters. J Biomed Mater Res B Appl Biomater 2004;70(2):286–96.
[62] Zong X, Ran S, Kim KS, Fang D, Hsiao BS, Chu B. Structure and morphology changes during in vitro degradation of electrospun poly(glycolide-*co*-lactide) nanofiber membrane. Biomacromolecules 2003;4(2):416–23.
[63] Parker GC, Anastassova-Kristeva M, Eisenberg LM, Rao MS, Williams MA, Sanberg PR, et al. Stem cells: shibboleths of development, part II: toward a functional definition. Stem Cells Dev 2005;14(5):463–9.
[64] Youn I, Choi JB, Cao L, Setton LA, Guilak F. Zonal variations in the three-dimensional morphology of the chondron measured in situ using confocal microscopy. Osteoarthritis Cartilage 2006;14(9): 889–97.
[65] Guilak F, Alexopoulos LG, Haider MA, Ting-Beall HP, Setton LA. Zonal uniformity in mechanical properties of the chondrocyte pericellular matrix: micropipette aspiration of canine chondrons isolated by cartilage homogenization. Ann Biomed Eng 2005;33(10): 1312–8.
[66] Poole CA, Ayad S, Gilbert RT. Chondrons from articular cartilage V. Immunohistochemical evaluation of type VI collagen organisation in isolated chondrons by light, confocal and electron microscopy. J Cell Sci 1992;103(Part 4):1101–10.
[67] Nishido TYK, Otori T, Desaki J. The network structure of corneal fibroblasts in the rat as revealed by scanning electron microscopy. Invest Ophthalmol Vis Sci 1988;29:1887–990.

[68] Marion NWLW, Reilly GC, Day DE, Rahaman MN, Mao JJ. Borate glass supports the in vitro osteogenic differentiation of human mesenchymal stem cells. Mech Adv Mater Struct 2005;12:1–8.
[69] Yourek GAA, Patel R, McCormick S, Reilly GC, Mao JJ. Nanophysical properties of living cells: the cytoskeleton. In: Dutta M, Stroscio M, editors. Biological nanostructures and applications of nanostructures in biology: electrical, mechanical, and optical properties. New York, NY: Kluwer Academic Publishing; 2004. p. 69–97.
[70] Marion NW, Mao JJ. Mesenchymal stem cells and tissue engineering. In: Robert Lanza, Irina Klimanskaya (Eds.), Methods in enzymology. Elsevier/Academic Press, 2006, in press.